Experimental study of a pre-compressed self-centering brace

Akbar Shahiditabar* and Hamid Moharrami*

School of Civil and Environmental Engineering, Tarbiat Modares University, Nasr, Jalal Ale Ahmad, Tehran, Islamic Republic of Iran

Several self-centering systems have been developed and tested so far, and all of them confront problems. Several problems like stress relaxation, elongation capacity and high post-yield stiffness are some of the problems, which should be addressed. The aim of this study is to find a solution to these problems. To this end, a new pre-compressed self-centering system has been proposed, tested and studied. Pre-compressed springs have been used to provide the required restoring force. Since the spring is under pressure and it has a high elastic capacity, the problem related to limited elongation capacity no longer exists. The experimental result indicates that the proposed self-centering brace has complete self-centering behaviour and low post-yield stiffness. The proposed self-centering system produces less secondary stiffness compared to other systems. The effect of secondary stiffness on the drift and base shear was studied. Results of the numerical models indicate that high secondary stiffness does not decrease the drift of the structure, it only increases the base shear. Therefore, to attain an economical design, using the proposed self-centering system with slight secondary stiffness is suggested.

Keywords: Bracing, earthquake, pre-compression, self-centering, spring, steel structures.

CONVENTIONAL lateral load-resisting systems are usually used to save lives during earthquakes[1,2]. However, less attention is paid to the performance of the structures. After a moderate earthquake, there is not much loss of lives, but cost of repair of the structures is high. A study on post-earthquake structures shows that if the residual drift is more than 0.6%, the cost of repair becomes higher than the cost of re-building the structures[3]. In addition, the performance of a structure after earthquake is important, because it is expected that some structures such as hospitals and schools continue to function after the earthquake. These concerns have led to the emergence of the performance-based design method. In this approach, a structure is designed so that it behaves as expected. The design of structures for immediate operation after an earthquake has its own requirements. One of the essential requirements is the elimination of residual drift.

*For correspondence. (e-mail: a_shahiditabar@yahoo.com; hamid@modares.ac.ir)

To address the design requirement of structures, self-centering systems have been proposed by various researchers. The ordinary lateral force-resisting systems such as moment frame and braced frame have rectangular-shaped hysteretic cycles which dissipate a considerable amount of energy during structure excitation, but they are prone to residual drift after an earthquake. Erochko *et al.*[4] concluded that buildings with a ductile steel yielding system are prone to experience more than 0.6% residual drift. Therefore, these types of structures need a self-centering system. Some of the self-centering systems have been briefly discussed by Filiatrault *et al*.[5].

A structure equipped with the self-centering system has the following advantages:

The self-centering system prevents the structure from experiencing residual drift after the earthquake.

Due to elimination of residual drifts, the P–Δ effect which is a cumulative effect of drift is also eliminated. In other words, the self-centering system makes the structure return to its original position after each cycle and prevents cumulative drift in the structure.

Some researchers have used pre-tensioned cables to re-centre the various types of structures[6–11]. For re-centering, the cables should simultaneously satisfy three conditions. (i) Cables should have sufficient elastic capacity to remain in the elastic range under imposed deformation. Since the elastic strain of cables is limited, their length should be sufficient to supply the elastic demand. (ii) Pre-tensioning force should be high enough to overcome friction (yield) force. To develop sufficient pre-tension force, a portion of the elastic capacity of the cable should be used. (iii) Since cables are tension-only elements and cannot bear pressure load, and an earthquake is a reciprocating motion, the development of a mechanism to induce just tension in the cables regardless of movement direction is necessary.

Several self-centering systems have been proposed and tested by researchers for a braced frame. A friction spring seismic damper has been studied by Filiatrault *et al.*[12]. In his model, the pre-compressed spring returns the structure to its initial configuration, but its elastic elongation capacity is not sufficient and corresponds to 1% storey drift. Another self-centering system has been developed by Zhu and Zhang[13]. Their main energy-dissipating component has been made of super-elastic Nitinol wires; however, the axial load capacity is not sufficient.

Christopoulos *et al.*[14] have developed a mechanism in which energy is dissipated by friction and pre-tensioned tendons are applied to return the structure to its initial shape. Although the elongation capacity of applied tendons was 2.3%, they just remained in the elastic range up to 2% storey drift. In larger drifts, when the frame is loaded beyond the cable elongation capacity, the cable gently fails. So, the self-centering characteristic is lost and the frame system is converted to a friction-only system. Therefore, frame strength decreases. To address this weak point, another mechanism has been developed[15], in which an intermediate element is applied to double the elongation capacity. Although applying the intermediate element doubles its length, it complicates the fabrication procedure and requires special care in construction and assembly[16].

In most of the current self-centering mechanisms, the pre-tensioned cable is used to self-centre the structure[17]. To achieve full self-centering characteristics, the pre-tension load of the cable should be greater than the friction slip (yield) force[14]. In the design process, the pre-tension force of the cable is deemed slightly greater than the friction slip force and stress relaxation of the cable is not involved in the design procedure. Previous studies have shown that the amount of stress relaxation is high enough to affect the performance of the structure during its life. Bazant and Yu[18] have demonstrated how stress relaxation caused problems in a box girder bridge.

In several studies, stress relaxation of steel has been evaluated at constant temperature and constant strain; however, studies on bridges around the world have proven the weakness of these assumptions. Stress relaxation is a viscoplastic phenomenon which is affected by variation in temperature. For example, at 20°C, it lasts 100 years to lose 13% of its initial pre-stress force, whereas it takes just 4 years to lose the same at 40°C. A study of the Koro-Babeldaob Bridge indicated that the pre-stress load loss of its cable was approximately 50% over 19 years[19]. Therefore, in usual building structures where pre-stressed cables may be exposed to sunlight or varying temperature, intensification of stress relaxation is expected. To overcome this problem, two solutions are available.

The first solution is increasing the pre-stress force to remedy stress loss due to relaxation. Increasing pre-stress force compensates the lack of pre-stress force over time. However, it stiffens the structure and also induces greater forces in other elements and makes the structure experience higher acceleration during the earthquake and increases post-yield stiffness[12,20,21]. So, increasing pre-stress force is not a rational and economic solution.

The second solution is the continuous inspection of pre-stressed cables. In this case, stress relaxation of the cable should be controlled continuously such that the pre-stress force becomes slightly more than the friction slip force. Owing to cable embedment in the wall and high maintenance cost, this is not a good solution. Consequently, cable stress relaxation is still a problem that should be studied comprehensively[14].

To address these drawbacks and restrictions, in this study a compression spring is used instead of the tension cable. The spring acts in compression and owing to its high elastic capacity, a short length of spring (compared to the cable) can easily provide the shortening capacity. Using some disc springs in parallel and in series to self-centre the system is another solution[22–25], whereas a large contact friction force between disc springs will result in small residual deformation[26]. However, stress relaxation needs to be studied in more detail in the future.

Here, a new pre-compressed self-centering braced frame is introduced. Its characteristics have been extracted by experiment and its effect on behaviour of the structure is studied numerically. It has been designed such that its hysteretic behaviour has a lower post-yield stiffness compared to other self-centering braces. This design does not affect the drift, but it reduces the base shear.

Mechanism of the pre-compressed self-centering brace

The proposed self-centering system uses pre-compressed springs for returning the structure to its original position. Since friction has stable energy dissipation, it is used for dissipating earthquake-induced energy[27]. Since the springs is presumed to be only in compression, providing a mechanism which keeps it always compressed, regardless of the direction of motion of the structure, is necessary. Mechanism of the proposed brace shown in Figure 1, keeps the spring in compression when the brace is subjected to either tension or compression.

The spring is pre-compressed by force P and placed between two end plates. The end plates are in contact with the inner and outer elements (but not welded to them). A friction device is used to dissipate energy (Figure 1 *a*).

Then a force T is applied to the brace, the inner element initiates to move to the right side while the applied force T overcomes the total value of the pre-compression force P plus the friction force F ($T = F + P$). In this condition, the stiffness of the brace reduces to the axial stiffness of the pre-compressed springs (Figure 1 *b*).

Now, the brace is under the load T with displacement δ to the right. To make the inner element return to its original position, the friction device should start moving to the left. To this end, a load $2F$ should be applied to the friction device in the opposite direction. In other words, while the brace is unloaded up to $2F$, the inner element initiates to move to its initial position and the axial stiffness of the brace is equal to the axial stiffness of the pre-compressed spring (Figure 2). Then, force T is

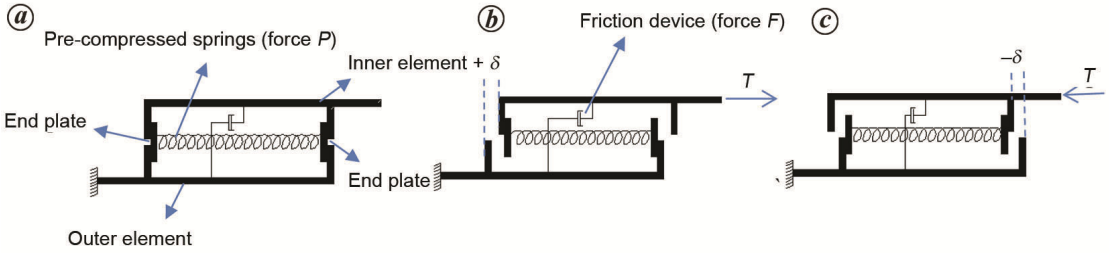

Figure 1 *a*–*c*. Mechanism of pre-compressed self-centering brace.

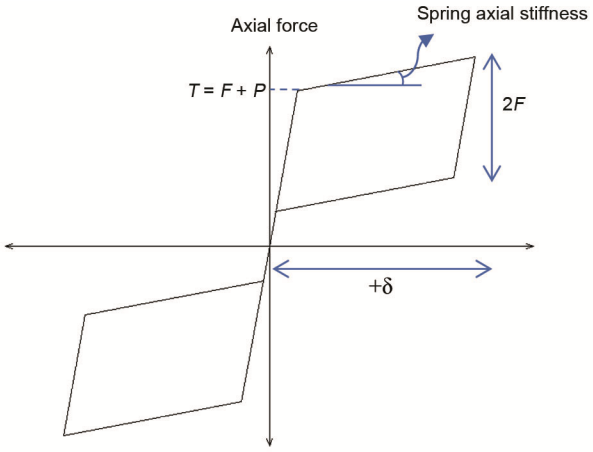

Figure 2. Flag-shaped response of self-centering brace.

applied to the brace in the opposite direction and the brace will show the same behaviour (Figure 1 *c*).

This self-centering mechanism which is applied in the brace is composed of two tubes. One in the other and the pre-compressed spring is located between the two tubes. To dissipate earthquake-induced energy, a friction device is used. The friction device includes two contact plates welded to the inner and outer tubes. When relative motion occurs between the inner and outer tubes, initially friction dissipates energy. The compression force between the two friction plates is provided by pre-tensioned bolts.

Spring axial test

To supply the required characteristics of the spring as specified by EN 10089 51CrV4, an ultra-heavy industrial spring was used[28]. This spring has been tested in the laboratory and Table 1 shows the test results.

Design of brace for a given load

For greater axial loads, a stronger spring should be designed and used in the brace. For strong earthquakes, the axial load induced in lateral load-resisting elements is much more than that of the tested spring. Therefore, to provide greater force and deformation, a spring with a larger dimension should be designed, fabricated and used. Based on DIN 2090 (ref. 28), capacity and axial stiffness of a compression spring are determined as follows

$$P = \frac{bh\sqrt{bh}}{\psi D_{\mathrm{m}}}\tau, \tag{1}$$

$$k = \frac{b^2h^2G}{\varepsilon D_{\mathrm{m}}^3 i_t}, \tag{2}$$

where τ is the induced shear stress, k the axial stiffness, D_{m} the mean coil diameter, i_{f} the number of active spring turns, G the modulus of elasticity in shear, and ψ and ε are shear coefficient and elasticity coefficient dependent on b/h.

For a greater load such as a load 300 kN, two points should be taken into account. First, dimensions of the tested spring, b, h and D shall be 3.3 times the tested spring. Second, to provide a low axial stiffness, it should be assumed four times.

It should be noted that in order to prevent longer spring from buckling, lateral supports must be provided at specific places[28–30].

In this study, since a single convenient spring was not available, to prepare the brace for the test, 12 springs were used in two different combinations and two specimens were fabricated and tested.

First specimen

In the first specimen, 12 springs were applied in parallel. The stiffness and ultimate capacity of this combination are as follows

$$P_{\text{assembly}} = 12P_{\text{tested spring}} = 12\times 27 = 324\ \text{kN}, \tag{3}$$

$$k_{\text{assembly}} = 12k_{\text{tested spring}} = 12\times 0.386\frac{\text{kN}}{\text{mm}} = 4.63\frac{\text{kN}}{\text{mm}}. \tag{4}$$

Twelve springs were placed between two end plates which were used to pre-press the springs. Therefore, they

Table 1. Characteristics of the spring

Dimensions (mm)			Experimental results (ultimate values)			
b	*h*	*D*	Length	Axial force *P* (kN)	Deformation (mm)	Axial stiffness (kN/mm)
11.8	13.5	50	305	27	70	0.386

b and *h* are dimensions of the rectangular cross-section of the spring and *D* is external coil diameter of the spring.

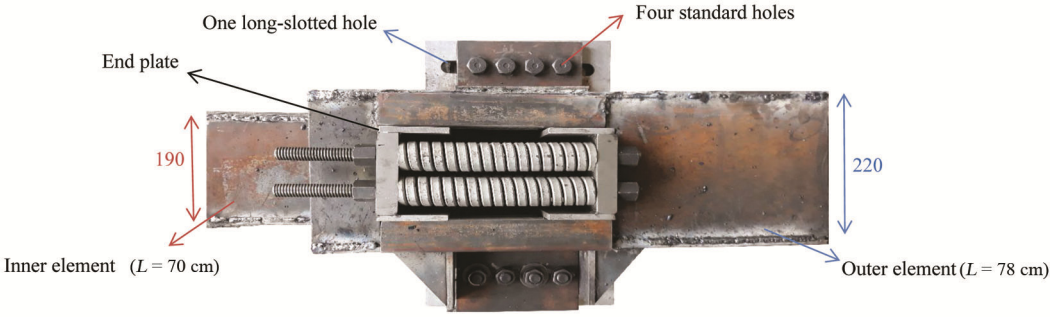

Figure 3. Pre-compressed spring inside two steel elements.

should be able to carry the pre-compression force. Also, the end plates and pre-pressed springs were located inside the self-centering element such that the former was in contact with either the inner or outer element when there is relative motion between the elements. Thus, the end plates should be able to carry the ultimate compression force of the springs within all support conditions. To achieve this goal, the cross-section of the end plate was calculated and fabricated.

Since the springs are in compression, to prevent them from bucking and misalignment, lateral support was provided by a rod placed concentrically inside the springs. The ends of the rods were attached to the end plate on one side and were free to move on the other. The initial length of the spring was 305 mm. To provide the pre-compression force, the springs were pre-pressed up to 30 mm, and placed inside two steel tubes (Figure 3).

The end plates located inside the steel tubes act as a guiding element. While relative motion between the two steel tubes initiated, the two end plates prevent misalignment of the steel tubes and guide them to move along the axis of the specimen. During relative motion, to minimize friction between the end plates and the steel tubes, their contact surfaces were shaped into a semi-circle. Thus, the friction is minimized and the contact surfaces behave as a guiding element.

For energy dissipation, two friction devices were used symmetrically on both sides of the self-centering element (Figure 3).

To fabricate the friction device, two plates were welded to two steel elements at both sides and a friction pad was used between the welded plates (Figure 3). To provide the compression force, four high-strength bolts M20 pre-stressed were used. Four standard holes in one plate and a long-slotted hole in the another plate were created to allow relative movement between the two plates. To dissipate energy, four friction pads of 5 mm diameter were used in the specimen.

Axial test of the first specimen: In the next step, the prepared specimen was tested under axial loading. In the specimen, 12 springs act in parallel. For the self-centering action, the springs were pre-stressed up to 110 kN. To achieve full re-centering behaviour, the pre-compression force should be able to overcome the friction force. Therefore, the friction force should be lower than 110 kN. Consequently, the specimen was tested for two different values of friction: 60 and 110 kN (Figure 4).

As seen in Figure 4, the brace is pushed up to 25 mm and it shows full self-centering behaviour for both friction capacities. As expected, the rate of increase in specimen capacity after yielding for both tests is proportional to the axial stiffness of the springs (4.6 kN/mm).

Second specimen

In the second specimen, 12 springs were used; four springs in series in three parallel positions (Figure 5).

The stiffness and ultimate capacity of this combination are as follows

$$P_{\text{assembly}} = 3P_{\text{tested spring}} = 3\times 27 = 81\,\text{kN}, \quad (5)$$

$$k_{\text{assembly}} = \frac{3}{4}k_{\text{tested spring}} = \frac{3}{4}\times 0.386\frac{\text{kN}}{\text{mm}} = 0.289\frac{\text{kN}}{\text{mm}}. \quad (6)$$

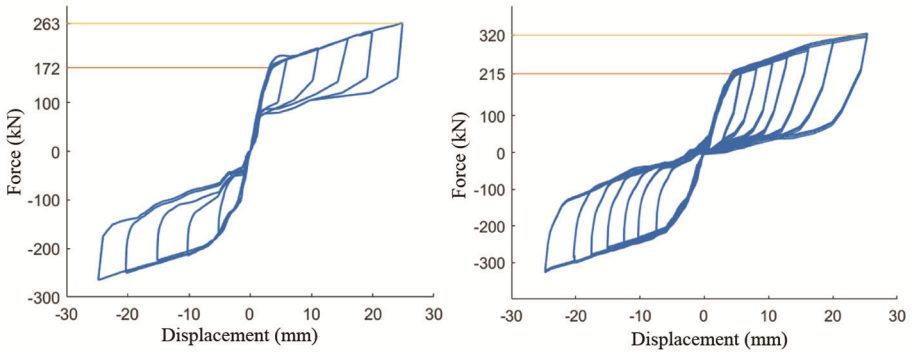

Figure 4. Hysteretic behaviour of the first specimen under quasi-static loading for two friction capacities: 60 and 100 kN.

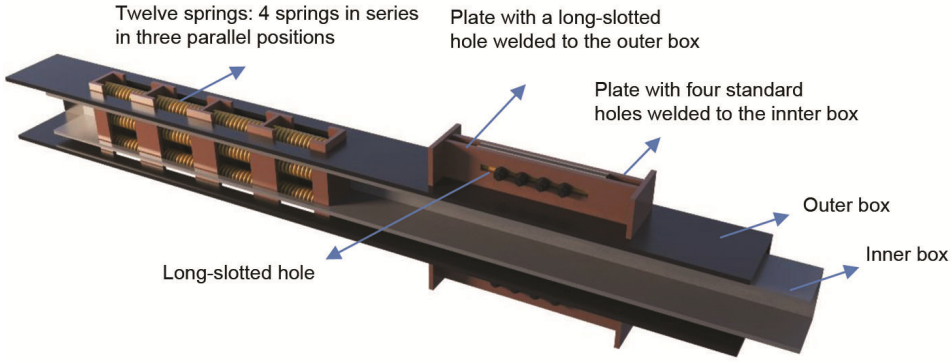

Figure 5. Quasi-static axial test of self-centering brace.

The stiffness of the assembly becomes equal to 3/4 of a single spring, i.e. the ultimate capacity of the assembly becomes three times the capacity of one spring while it tolerates a deformation up to four times the ultimate deformation of the spring.

Other components of the second specimen such as friction device, end plates and lateral supports of the springs were the same as in the first specimen. The overall length of the specimen was 230 cm. It was composed of two steel elements with rectangular tubular of different sizes. One of the tubular steel elements was smaller than the other one and it was located inside the bigger one that was fitted concentrically. Twelve springs and two friction devices at the two opposite sides of the brace completed the device. The two plates were welded to two steel elements on both sides and a friction pad was used between the two plates. To provide the compression force, four pre-stressed bolts were used and to allow relative movement between the two plates, standard holes in one plate and a long-slotted hole in the other plate were made.

In the specimen, 12 springs have been used for the action of self-centering. Since three springs are in parallel, according to eq. (3), the ultimate axial capacity of the assembly is 81 kN. These springs are pre-loaded up to $P = 39$ kN. To achieve full re-centering behaviour, the pre-compression force should be able to overcome the friction force. Therefore, the friction force should be lower than 39 kN. This specimen was tested for two different values of friction capacity: 17 and 39 kN.

As seen in Figure 6, the brace is pushed up to 50 mm and it shows full self-centering behaviour for both friction capacities. As expected, the rate of increase in brace capacity after yielding for both tests is proportional to the axial stiffness of the springs. Since the axial stiffness of the springs is 289 N/mm, as seen in Figure 6, for a 50 mm displacement, there will be 14.5 kN increase in axial load.

The axial stiffness of the spring is proportional to its length and consequently different values of post-yield stiffness of the brace can be achieved. Thus the compression spring is capable of providing different values of post-yield stiffness.

Numerical modelling

To study the effects of post-yield stiffness on the behaviour of structures, three buildings with different number of stories, 4, 8 and 12 were used. Other characteristics of the buildings such as storey height, bay width, gravity

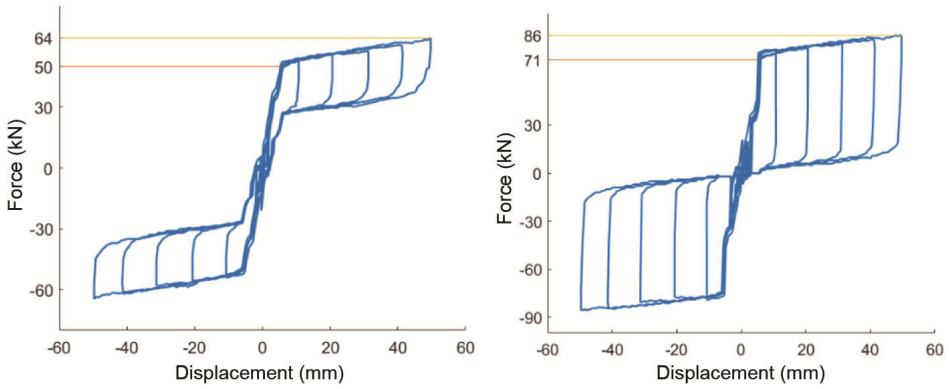

Figure 6. Hysteretic behaviour of the tested frame under quasi-static loading.

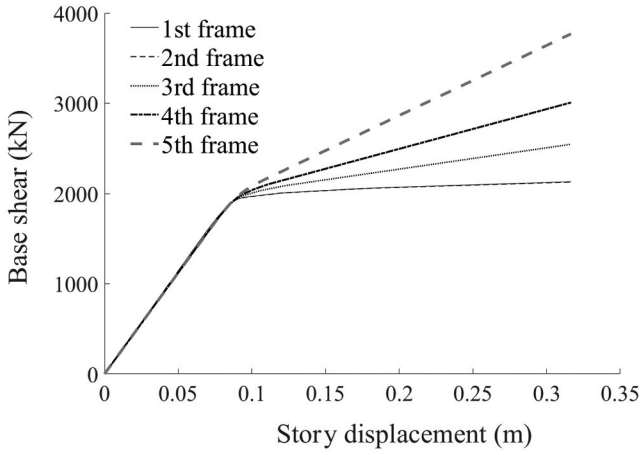

Figure 7. Secondary stiffnesses of five frames.

loading, seismic loading and storey plan were the same. Each building was designed in full compliance with the governing design requirements of ASCE7-16 (ref. 31).

The storey plan is of five bays in two orthogonal directions. Four diagonal bucking restrained braces (BRBs) located along the perimeter of the structure provided the lateral stiffness in each direction. All storeys are of constant height of 3.5 m and the span of all bays is 6 m.

Beam-column connections are assumed simple (non-moment resisting) in the design.

The loads used in the design of the structure are as follows: Distributed live load, partition load and snow load are assumed to be 2, 1 and 1 kN/m^2 respectively. Also, S_S and S_1 are assumed to be 2.4 and 0.83 respectively. Site class D is used for design. The assessment process begins with $R = 8$, $C_d = 5$ and $\Omega = 2.5$.

Since BRB frames are distributed symmetrically in the plan, the accidental torsion can be neglected and a 2D frame will be able to represent the behaviour of the structure[31].

The structure is of six frames in the X-direction. The frames located in axes A and B, including BRBs, are designed with similar elements, while other frames (1 to 4) are hinged. Consequently, the lateral stiffnesses of the frames A and B are similar and equal to half the lateral stiffness of the entire structure in the X-direction. Also, due to assigning rigid diaphragms at storey levels and uniform distributed loadings on the diaphragms, the effective masses of the 2D frames located in axes A and B are similar and half the effective mass of the entire structure. Consequently, the periods and mode shapes of the 2D frame located in either axes A or B and the entire structure become similar.

Numerical modelling is intended to study the effect of post-yield stiffness on the drift and the base shear of the structure. Since dynamic behaviour of the 2D frame located in axis A and that of the entire structure are similar, this 2D frame is able to reflect the behaviour of the entire structure. As a result, the 2D frame located in axis A is chosen for further analysis.

The structural analysis software selected for the study is the Open System for Earthquake Simulation (OpenSees). To model the elements, the fibre element that allows plasticity to spread throughout the elements is used.

To assess the effect of post-yield stiffness of the self-centering brace, BRB is replaced by a self-centering element[32] and the frame is studied for four different values of secondary stiffness. Therefore, the frame is studied in five different models. In the first model, the frame with BRB is studied. In the second model, BRB is replaced by the corresponding self-centering brace in which secondary stiffness of the self-centering brace is equal to that of the BRB. In the third, fourth and fifth frames, secondary stiffness of the self-centering element becomes 2, 4 and 8 times that the self-centering element of the second frame. Figure 7 shows the force–displacement plots for the models.

To perform nonlinear seismic analysis, a nonlinear response history was used. In this regard, seven ground motions were selected from actual recorded events (Table 2).

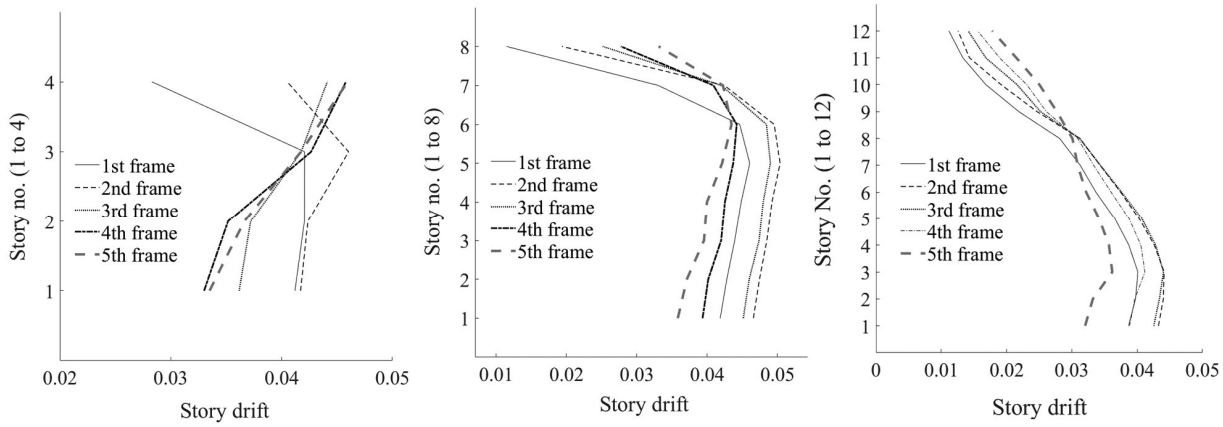

Figure 8. Storey drift of five frames with 4, 8 and 12 stories under dynamic loading.

Table 2. The selected ground motion records

Record no.	Earthquake	Station	Magnitude
1	Superstition Hills	Poe road (temp)	6.5
2	Friuli	Tolmezzo	6.5
3	Imperial Valley	Arcelik	7.5
4	Taiwan (Chi-Chi)	TCU045	7.6
5	Loma Prieta	Capitola	6.9
6	Landers	TCU045	7.6
7	Northridge	Poe Road (temp)	6.5

Table 3. Base shear (kN) of five frames under dynamic loading

Storey	First frame	Second frame	Third frame	Fourth frame
4	2427	2163	2659	3469
8	4057	4400	4654	6977
12	6282	7088	7279	8054

To observe the effect of secondary stiffness on drift and base shear, the models were subjected to seven scaled records. Due to the use of a suite of seven ground motions, the average of responses was utilized to compare the behaviour of the structures.

As seen in Figure 8, generally, with increase in the secondary stiffness of the self-centering elements, storey drift decreases. However, the reverse can be seen for the top four storeys of the 12-storey frame. As a result, increasing secondary stiffness does not always help to decrease storey drift. Christopoulos *et al.*[33] studied the seismic response of self-centering SDOF systems and concluded that increasing the secondary stiffness of the system does not lead to a reduction in storey displacement. Zhang *et al.*[34] have shown that small positive secondary stiffness has relatively less influence on the displacement of the SDOF system. Hu and Zhang[35] have studied the effect of post-yield stiffness on partially self-centering SDOF systems. Table 3 shows that an increase in secondary stiffness of the self-centering system increases the base shear. Consequently, using a self-centering element with high post-yield stiffness is not recommended, because it induces greater force in force-controlled elements.

Huang *et al.*[36] showed that for low-rise buildings higher cost of self-centering brace can be compensated for lower earthquake-induced losses to the building, provided that the force control elements of the self-centered frame and that without a self-centering system are the same. A review of previous studies shows that most of the self-centering systems are proposed with high secondary stiffness. However, the present study proposes low secondary stiffness for self-centering systems because it is more practical and economical.

Actual size brace with low post-yield stiffness

To show the novelty of the proposed self-centering brace, an actual size brace is designed based on the experimental results. To this end, it is assumed that the overall length of the brace is 6 m and it should tolerate an axial force 600 kN. A pre-compressed spring with length 4 m can be placed in the brace. Moreover, to guarantee the self-centering behaviour of the brace, the pre-compression force should not be smaller than the friction force. Therefore, friction should bear 300 kN and the spring should be pre-compressed at least up to 300 kN. In addition, the pre-compressed springs will tolerate a greater force and deformation while the brace initiates motion. So, half the ultimate capacity of the spring is suggested to be used as the self-centering force and the rest is used for the post-yield phase. Two of the designed springs are used in parallel (eqs (1) and (2)). The axial stiffness of these two springs in parallel is as follows

$$k_{\text{eq}} = n \times 3.185 \frac{\text{kN}}{\text{cm}} = 6.39 \frac{\text{kN}}{\text{cm}}, \tag{7}$$

where n is the number of springs in parallel.

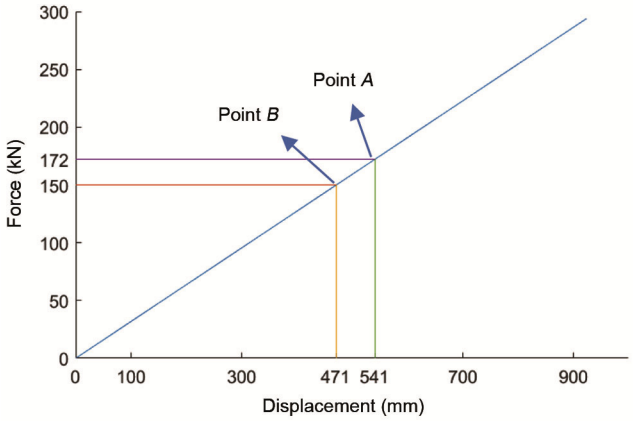

Figure 9. Axial behaviour of the actual size spring.

Figure 9 shows the expected behaviour of the spring under axial load.

The spring is pre-compressed up to point *A* to provide the required self-centering force and when it experiences deformation up to point *B* (i.e. 7 cm axial deformation), its axial force reaches 172 kN (Figure 9). Therefore, the axial force of the brace in the post-yield phase increases from 600 (600 = 300 + 300) to 644 kN (644 = 300 + 2 × 172). In other words, the axial force of the brace increases by approximately 7% in the post-yield phase.

Post-yield stiffness of the proposed self-centering brace is smaller than that of a steel BRB. For conventional steel braces, post-yield stiffness is 3% of the initial value[37]. A BRB of length 6 m with $F_y = 24$ kN/cm^2, designed to yield at 600 kN, should have a cross-sectional area equal to 25 cm^2. Therefore, post-yield stiffness of this BRB is

$$k_{\text{secondary}} = 0.03\frac{EA}{L} = 0.03\times\frac{2e7\times 25}{600} = 25\frac{\text{kN}}{\text{cm}}. \quad (8)$$

Under deformation of 7 cm, the axial force of the BRB increases to $25 \times 7 = 175$ kN. Consequently, secondary stiffness of the proposed self-centering brace is even smaller than that of BRB, and it is practical and economical to be applied.

Conclusion

Usually, pre-stressed cables are used to provide restoring forces for the self-centering mechanism that makes the structures return to their original position after every loading cycle. The pre-stressed cable confronts three problems: first, stress relaxation that causes restoring force of the cable to decrease over time; second, the low elastic capacity of cables that necessitates long cables for satisfying the allowable drifts, and third, the self-centering system produces high post-yield stiffness.

In this study, to remove the above-mentioned drawbacks, a pre-compressed self-centering mechanism has been proposed and tested. A pre-compressed spring has been used to act as a restoring force. The behaviour of the spring under quasi-static loading was tested in the laboratory. Experimental results and analytical calculations proved that the proposed compression spring has low secondary stiffness.

The effect of post-yield stiffness of the self-centering system on the drift and base shear was examined. The results of numerical modelling indicate that post-yield stiffness does not affect the drift but increases the base shear considerably. Accordingly, it was concluded that the self-centering system with small secondary stiffness is better than that with high secondary stiffness.

Numerical examples show that the secondary stiffness of a self-centering system affect the base shear, and consequently, the internal forces in the structural elements. As a result, for equal drift, the proposed mechanism that has a small secondary stiffness produces less force in structural elements compared to self-centering systems with high secondary stiffness. This characteristic of the proposed self-centering system makes it cost-effective.

1. Pandikkadavath, M. S. and Sahoo, D. R., Analytical investigation on cyclic response of buckling-restrained braces with short yielding core segments. *Int. J. Steel Struct.*, 2016, **16**(4), 1273–1285.
2. Ghowsi, A. F. and Sahoo, D. R., Effect of loading history and restraining parameters on cyclic response of steel BRBs. *Int. J. Steel Struct*, 2018, **19**, 1055–1069.
3. McCormick, J., Aburano, H., Ikenaga, M. and Nakashima, M., Permissible residual deformation levels for building structures considering both safety and human elements. In 14th World Conference on Earthquake Engineering, Beijing, China, 2008.
4. Erochko, J., Christopoulos, C., Tremblay, R. and Choi, H., Residual drift response of SMRFs and BRB frames in steel buildings designed according to ASCE 7-05. *J. Struct. Eng.*, 2011, **137**(5), 589–599.
5. Filiatrault, A., Restrepo, J. and Christopoulos, C., Development of self-centering earthquake resisting systems. In 13th World Conference on Earthquake Engineering, Vancouver, BC, Canada, 2004.
6. Keivan, A. and Zhang, Y., Nonlinear seismic performance of *Y*-type self-centering steel eccentrically braced frame buildings. *J. Eng. Struct*., 2019, **179**, 448–459.
7. Gu, A., Zhou, Y., Xiao, Y., Li, Q. and Qu, G., Experimental study and parameter analysis on the seismic performance of self-centering hybrid reinforced concrete shear walls. *Soil Dyn. Earthquake Eng.*, 2019, **116**, 409–420.
8. Du, X., Wang, W. and Chan, T. M., Seismic design of beam-through steel frames with self-centering modular panels. *J. Construct. Steel Res.*, 2018, **144**, 179–188.
9. Song, L. L., Guo, T. and Cao, Z. L., Seismic response of self-centering prestressed concrete moment resisting frames with web friction devices. *Soil Dyn. Earthq. Eng.*, 2015, **71**, 151–162.
10. Kamperidis, V. C., Karavasilis, T. L. and Vasdravellis, G., Self-centering steel column base with metallic energy dissipation devices. *J. Construct. Steel Res.*, 2018, **149**, 14–30.
11. Chung, C. C., Wen, T. J. and Ping, C. T., Development and validation tests of a dual-core self-centering sandwiched buckling-restrained brace (SC-SBRB) for seismic resistance. *Eng. Struct.*, 2016, **121**, 30–41.

12. Filiatrault, A., Tremblay, R. and Kar, R., Performance evaluation of friction spring seismic damper. *J. Struct. Eng.*, 2000, **126**, 491–499.
13. Zhu, S. and Zhang, Y., Seismic behaviour of self-centering braced frame buildings with reusable hysteretic damping brace. *Earthq. Eng. Struct. Dyn.*, 2007, **36**, 1329–1346.
14. Christopoulos, C., Tremblay, R., Kim, H.-J. and Lacerte, M., Self-centering energy dissipative bracing system for the seismic resistance of structures: development and validation. *J. Struct. Eng.*, 2008, **134**(1), 96–107.
15. Erochko, J., Christopoulos, C. and Tremblay, R., Design and testing of an enhanced-elongation telescoping self-centering energy-dissipative brace. *J. Struct. Eng.*, 2014, **141**(6), 1–11.
16. Chi, P., Guo, T., Peng, Y., Cao, D. and Dong, J., Development of a self-centering tension-only brace for seismic protection of frame structures. *J. Steel Compos. Struct.*, 2018, **26(**5).
17. López-Barraza, A., Ruiz, S. E., Reyes-Salazar, A. and Bojórquez, E., Demands and distribution of hysteretic energy in moment resistant self-centering steel frames. *J. Steel Compos. Struct.*, 2016, **20**(5), 1155–1171.
18. Bazant, Z. P. and Yu, Q., Relaxation of prestressing steel at varying strain and temperature: viscoplastic constitutive relation. *J. Eng. Mech.*, 2013, **139(**7), 814–823.
19. Bažant, Z. P., Yu, Q. and Li, G.-H., Excessive long-time deflections of prestressed box girders. I: record-span bridge in Palau and other paradigms. *J. Struct. Eng.*, 2012, **138**(6), 676–686.
20. Tremblay, R., Lacerte, M. and Christopoulos, C., Seismic response of multistory buildings with self-centering energy dissipative steel braces. *J. Struct. Eng.,* 2008, **134**(1), 108–120.
21. Morelli, F., Piscini, A. and Salvatore, W., Seismic behavior of an industrial steel structure retrofitted with self-centering hysteretic dampers. *J. Construct. Steel Res.*, 2017, **139**, 157–175.
22. Latour, M., Rizzano, G., Santiago, A. and Silva, L. S. D., Experimental response of a low-yielding, self-centering, rocking column base joint with friction dampers. *Soil Dyn. Earthq. Eng.*, 2019, **116**, 580–592.
23. Xu, L., Xiao, S. and Li, Z., Hysteretic behavior and parametric studies of a self-centering RC wall with disc spring devices. *Soil Dyn. Earthq. Eng.*, 2018, **115**, 476–488.
24. Xu, L., Yao, S. and Sun, Y., Development and validation tests of an assembly self-centering energy dissipation brace. *Soil Dyn. Earthq. Eng.*, 2019, **116**, 120–129.
25. Xu, L., Liu, J. and Li, Z., Behavior and design considerations of steel plate shear wall with self-centering energy dissipation braces. *J. Thin-Walled Struct.*, 2018, **132**, 629–641.
26. Xu, L.-H., Fan, X.-W. and Li, Z.-X., Development and experimental verification of a pre-pressed spring self-centering energy dissipation brace. *J. Eng. Struct.*, 2016, **127**, 49–61.
27. Xu, L., Fan, X., Lu, D. and Li, Z., Hysteretic behavior studies of self-centering energy dissipation bracing system. *J. Steel Compos. Struct.*, 2016, **20**(6), 1205–1219.
28. DIN 2090, Standard: Helical Compression springs made of flat bar steel, Calculation, German, 1971–01.
29. BS EN 10089, Hot rolled steels for quenched and tempered springs. Technical delivery conditions, British-Adopted European Standard, 2002.
30. Budynas, R. G. and Nisbett, J. K., *Shigley's Mechanical Engineering Design*, McGraw-Hill, NY, USA, 2009, 9th edn.
31. ASCE 7-16, Minimum design loads and associated criteria for buildings and other structures, American Society of Civil Engineers, 2016.
32. Tian, L. and Qiu, C., Modal pushover analysis of self-centering concentrically braced frames. *J. Struct. Eng. Mech.*, 2018, **65(**3), 251–261.
33. Christopoulos, C., Filiatrault, A. and Folz, B., Seismic response of self-centering hysteretic SDOF systems. *Earth. Eng. Struct. Dyn.*, 2002, **31**, 1131–1150.
34. Zhang, C., Steele, T. C. and Wiebe, L. D., Design-level estimation of seismic displacements for self-centering SDOF systems on stiff soil. *J. Eng. Struct.*, 2018, **177**, 431–443.
35. Hu, X. and Zhang, Y., Ductility demand of partially self-centering structures under seismic loading: SDOF systems. *J. Earthq. Struct.*, 2013, **4**(4).
36. Huang, Q., Dyanati, M., Roke, D. A., Chandra, A. and Sett, K., Economic feasibility study of self-centering concentrically braced frame systems. *J. Struct. Eng.*, 2018, **144**(8), 1–15.
37. ASCE-SEI 41-17, Seismic evaluation and retrofit of existing buildings, American Society of Civil Engineers, 2017.

Received 4 August 2019; revised accepted 5 March 2020

doi: 10.18520/cs/v119/i1/59-67